0026-895X/01/5903-506–513$3.00
MOLECULAR PHARMACOLOGY
Copyright © 2001 The American Society for Pharmacology and Experimental Therapeutics
Mol Pharmacol 59:506–513, 2001

Vol. 59, No. 3
541/883036
Printed in U.S.A.

A Bioactive Metabolite of Benzo[*a*]pyrene, Benzo[*a*]pyrene-7,8-dione, Selectively Alters Microsomal Ca^{2+} Transport and Ryanodine Receptor Function

ISAAC N. PESSAH, CHRIS BELTZNER, SCOTT W. BURCHIEL, GOPISHETTY SRIDHAR, TREVOR PENNING, and WEI FENG

Department of Molecular Biosciences, School of Veterinary Medicine, University of California, Davis, California (I.N.P., C.B., W.F.); College of Pharmacy Toxicology Program, The University of New Mexico, Albuquerque, New Mexico (S.W.B.); and Department of Pharmacology, University of Pennsylvania, Philadelphia, Pennsylvania (G.S., T.P.)

Received August 31, 2000; accepted November 7, 2000

This paper is available online at http://molpharm.aspetjournals.org

ABSTRACT

Polycyclic aromatic hydrocarbons are environmental pollutants known to be carcinogenic and immunotoxic. In intact cell assays, benzo[*a*]pyrene (B[*a*]P) disrupts Ca^{2+} homeostasis in both immune and nonimmune cells, but the molecular mechanism is undefined. In this study, B[*a*]P and five metabolites are examined for their ability to alter Ca^{2+} transport across microsomal membranes. Using a well-defined model system, junctional SR vesicles from skeletal muscle, we show that a single *o*-quinone metabolite of B[*a*]P, B[*a*]P-7,8-dione, can account for altered Ca^{2+} transport across microsomal membranes. B[*a*]P-7,8-dione induces net Ca^{2+} release from actively loaded vesicles in a dose-, time-, and Ca^{2+}-dependent manner. In the presence of 5 μM extravesicular Ca^{2+}, B[*a*]P-7,8-dione exhibited threshold and EC_{50} values of 0.4 and 2 μM, respectively, and a maximal release rate of 2 μmol of Ca^{2+} min^{-1} mg^{-1}. The mechanism by which B[*a*]P-7,8-dione enhanced Ca^{2+} efflux was further investigated by measuring macroscopic fluxes and single RyR1 channels reconstituted in bilayer lipid membranes and direct measurements of SERCA catalytic activity. B[*a*]P-7,8-dione ($\leq$ 20 μM) had no measurable effect on initial rates of Ca^{2+} accumulation in the presence of ruthenium red to block ryanodine receptor (RyR1), nor did it alter Ca^{2+}-dependent (thapsigargin-sensitive) ATPase activity. B[*a*]P-7,8-dione selectively altered the function of RyR1 in a time-dependent diphasic manner, first activating then inhibiting channel activity. Considering that RyR1 and its two alternate isoforms are broadly expressed in mammalian cells and their important role in Ca^{2+}-signaling, the present results reveal a mechanism by which metabolic bioactivation of B[*a*]P may mediate RyR dysfunction of pathophysiological significance.

Polycyclic aromatic hydrocarbons (PAHs), such as benzo[*a*]pyrene (B[*a*]P), are ubiquitous environmental pollutants formed during the burning of fossil fuels and combustion of other products, as well as during cooking (Baum, 1978). B[*a*]P is a complete carcinogen with both tumor-initiating and tumor-promoting properties (Ethier and Ullrich, 1982). For tumor initiation, carcinogenic PAHs seem to require bioactivation by either a family of cytochrome P450s or aldo-keto reductases to form DNA-reactive metabolites (Dipple, 1994; Penning et al., 1999). B[*a*]P is also known to alter cell-signaling pathways associated with growth factor receptor-dependent cell proliferation and survival (Tannheimer et al., 1997, 1998), as well as cell to cell interactions (Upham et al., 1998). Carcinogenic PAHs are also immunotoxic at high doses. For example, B[*a*]P and 7,12-dimethylbenz[*a*]anthracene suppress humoral and cell-mediated immunity in mice (Davila et al., 1996, 1999).

Burchiel and coworkers have shown a correlation between the ability of PAHs to produce immunosuppression and their ability to elevate intracellular Ca^{2+}. B[*a*]P is one of several carcinogenic PAHs that increase intracellular Ca^{2+} in lymphoid (Mounho et al., 1997; Romero et al., 1997; Mounho and Burchiel, 1998) and nonlymphoid cells (Holsapple et al., 1996; Tannheimer et al., 1999). Several mechanisms have been shown to be responsible for altered Ca^{2+} homeostasis. In human T cells, such PAHs as dimethylbenz[*a*]anthracene have been found to activate *src*-related proto-oncogenes, leading to a rapid IP_3-dependent Ca^{2+} release from endoplasmic reticulum (Archuleta et al., 1993). However, because this

Supported by National Institutes of Health Grants ES05707and ES10173 (I.N.P.); ES07259 and ES05495 (S.W.B.), and CA39504 (T.M.P.).

ABBREVIATIONS: PAH, polycyclic aromatic hydrocarbon; B[*a*]P, benzo[*a*]pyrene; SERCA, sarcoplasmic/endoplasmic reticulum ATPase; CICR, Ca^{2+}-induced Ca^{2+} release; SR, sarcoplasmic reticulum; RyR, ryanodine receptor; DMSO, dimethyl sulfoxide; MOPS, potassium 3-(N-morpholino)propanesulfonic acid; B[*a*]P-7,8-diol, (±)-*trans*-7,8-dihydroxy-7,8-dihydro-benzo[*a*]pyrene; (±)-*anti*-BPDE, (±)- *anti*-7β,8α-dihydroxy-9α,10α-epoxy-7,8,9,10-tetrahydrobenzo[*a*]pyrene; RR, ruthenium red; AKR, aldo-ketoreductase; CPM, 7-diethylamino-3-(4′-maleimidylphenyl)-4-methylcoumarin; NQ, naphthalene-1,4-dione.

activity has been also seen by some noncarcinogenic PAHs, the specificity of this action is questioned (Davila et al., 1999). Further results indicated that immunotoxic PAHs, such as B[*a*]P, inhibited ATP-dependent $^{45}Ca^{2+}$ uptake into microsomal vesicles but not by the less immunotoxic compounds anthracene and benzo[*e*]pyrene. These effects correlated well with decreased SERCA-type Ca^{2+}-ATPase catalytic activity but affected neither Na^+/K^+-ATPase activity nor plasma membrane Ca^{2+}-ATPase activities (Krieger et al., 1995). However, recent work aimed at characterizing the interactions between PAHs and specific SERCA isoforms (including SERCA1, -2a, and -3) demonstrated that PAHs do not have a direct inhibitory effect on the cloned rat SERCAs expressed in human embryonic kidney 293 cells (Zhao et al., 1996). Although thapsigargin (100 nM) and 2,5-di(*t*-butyl)-1,4-benzohydroquinone (10 μM) completely inhibited each of the heterologously expressed SERCA isoforms, B[*a*]P and six related PAH structures failed to inhibit any SERCA activity at concentrations as high as 10 μM (Zhao et al., 1996). These results suggest that the Ca^{2+}-elevating activity of B[*a*]P and its known primary metabolites occurs independent of SERCA. Therefore alternate mechanisms may be involved in altered Ca^{2+} homeostasis.

Although B[*a*]P *o*-quinones derived from the *trans*-dihydrodiols have been shown to decrease cell viability and cause cell death, presumably by GSH depletion (Flowers-Geary et al., 1993, 1995), the underlying mechanism(s) are not understood. Because the cytoxicity of B[*a*]P *o*-quinones may be mediated via enzymatic one-electron redox cycling, we investigated the activity of B[*a*]P and five metabolites for their ability to alter Ca^{2+} transport across junctional sarcoplasmic reticulum (SR) membrane vesicles isolated from skeletal muscle. SR preparations serve as a suitable model to elucidate mechanisms of altered Ca^{2+} transport because they have a well-defined Ca^{2+} transport system. The SERCA-1 pump mediates Ca^{2+} sequestration, whereas Ca^{2+}-induced Ca^{2+} release (CICR) channels, also known as ryanodine receptors (RyR), mediate the release of stored Ca^{2+}. In light of the exquisite sensitivity of RyR to sulfhydryl reagents and redox-active quinones (Feng et al., 1999; Pessah and Feng, 2000) we investigated the hypothesis that RyR rather than SERCA may be a selective target for redox-active B[*a*]P *o*-quinones.

Materials and Methods

Preparation of SR Membranes. Sarcoplasmic reticulum (SR) membrane vesicles enriched in RyR type 1 (RyR1) and SERCA1 were prepared from back and hind limb skeletal muscles of New Zealand White rabbits according to the method of Saito et al. (1984). The preparations were stored in 10% sucrose, 5 mM imidazole, pH 7.4, at −80°C.

Ca^{2+} ATPase Activity. Rates of ATP hydrolysis were determined with a coupled enzyme assay measuring the oxidation of NADH as a linear decrease in absorbance at 340 nm (Schwartz et al., 1969). SR membrane vesicles (50 μg of protein) were added to the temperature-controlled cuvettes at 37°C. The cuvettes contained assay buffer consisting of 5 mM HEPES, pH 7.0, 100 mM KCl, 5 mM $MgCl_2$, 60 μM EGTA, 100 μM $CaCl_2$, 0.3 mM sucrose, 2 mM phospho(enol)pyruvate, 0.8 mM NADH, 24 U/ml lactate dehydrogenase, 16.8 U of pyruvate kinase, and 1.5 μg/ml of the Ca^{2+} ionophore A23187 (final volume, 1.2 ml). B[*a*]P or its derivatives were introduced into test cuvettes 2 min before the start of the reaction, whereas paired control reactions received an equivalent volume of solvent (DMSO). DMSO was ≤ 1% in the final assay medium. After zeroing the spectrophotometer, reactions were started by addition of 1 mM Na_2ATP and the total ATPase activity (measured as a linear decline in NADH absorbance) monitored for at least 30 s. The Ca^{2+}-independent (non-SERCA) component of ATPase activity was measured by the addition of either 4 mM K_2EGTA or 1 μM thapsigargin to the reaction mixture. Ca^{2+}-dependent rates were calculated as the difference between total ATPase and Ca^{2+}-independent rates.

Macroscopic Ca^{2+} Transport Measurement. Ca^{2+} transport across SR vesicles was measured with the membrane-impermeant Ca^{2+}-sensitive dye antipyrylazo III using a diode array spectrophotometer (model 8452; Hewlett Packard, Palo Alto, CA). Skeletal SR vesicles (42 μg/ml) were added to 1.15 ml of ATP-regenerating buffer consisting of 95 mM KCl, 20 mM MOPS, 7.5 mM sodium pryophosphate (Palade, 1987), 250 μM antipyrylazo III, 12 μg of creatine phosphokinase, 5 μM phosphocreatine, and 1 mM MgATP, pH 7.0 (final volume of 1.2 ml). Transport assays were performed at 37°C in temperature-controlled cuvettes with constant stirring. SR vesicles were loaded with seven sequential additions of 24 nmol of $CaCl_2$, which constituted approximately 80% of their loading capacity. Net Ca^{2+} fluxes across SR vesicles were measured by monitoring extravesicular changes in free Ca^{2+} by subtracting the absorbance of antipyrylazo III at 790 nm from absorbance at 710 nm at 2- to 4-sec intervals. At the end of each experiment, the total intravesicular Ca^{2+} was determined by addition of 3 μM A23187, a Ca^{2+} ionophore, and the absorbance signals were calibrated by addition of 12 or 24 nmol of $CaCl_2$ from a National Bureau of Standard stock solution. The actions of B[*a*]P and its derivatives were studied by adding the compound after the loading phase was complete in the presence or absence of known inhibitors or RyR and in the presence of 0.1 or 5 μM extravesicular free Ca^{2+}. None of the PAHs used in this study interfered with the absorbance properties or calibration of the antipyrylazo III dye.

Measurement of [^{3}H]Ryanodine-Binding and Data Analysis. SR membrane vesicles (25 μg of protein/ml) were incubated in the presence or absence of B[*a*]P-7,8-dione in assay buffer containing 2- mM HEPES, pH 7.1, 250 mM KCl, 15 mM NaCl, 50 μM $CaCl_2$, and [^{3}H]ryanodine (2 nM). Apparent association kinetics were determined in the presence and absence of B[*a*]P or B[*a*]P-7,8-dione and the binding reactions were quenched at times ranging between 5 min and 3 h by filtration through GF/B glass-fiber filters. The filters were washed twice with ice-cold harvest buffer, composed of 20 mM Tris-HCl, 250 mM KCl, 15 mM NaCl, and 50 μM $CaCl_2$, pH 7.1. Each assay was performed in duplicate and repeated at least twice. Nonspecific binding was determined by incubating SR vesicles in the presence of 1000-fold excess unlabeled ryanodine. Association kinetics were analyzed excluding the inhibition phase (when present) by fitting to a single exponential, and calculating the apparent association rate constant (k_{obs}) and apparent half-time ($T_{1/2}$) (ENZFITTER, Elsevier Biosoft, Cambridge, UK).

Single Channel Kinetics in Bilayer Lipid Membranes. RyR1 channels were reconstituted into artificial planar lipid bilayer (5:2 phosphatidylethanolamine/phosphatidylcholine, 60 mg/ml in decane) by introducing membrane vesicles to the *cis* chamber. The *cis* chamber contained 0.7 ml of 500 mM CsCl, 50 μM $CaCl_2$, and 10 mM HEPES, pH 7.4, whereas the *trans* side contained 100 mM CsCl, 50 μM $CaCl_2$, and 10 mM HEPES, pH 7.4. Upon the fusion of SR vesicle into bilayer, the *cis* chamber was perfused with the identical solution lacking $CaCl_2$. Single-channel activity was measured at a holding potential of +30 mV (applied *cis* relative to the *trans* ground side) using a patch-clamp amplifier (Dagan 3900). The data was filtered at 1 kHz before acquisition at 10 kHz by a DigiData 1200 (Axon Instruments, Foster City, CA). The data were analyzed using pClamp 7 (Axon Instruments) without additional filtering. Control data were obtained for at least 30 s before addition of the test compound. Once the test compound was present, data were collected for at least 10 min.

Chemical Reagents. Unless otherwise indicated, all reagents, including B[*a*]P, were obtained from Sigma-Aldrich (St. Louis, MO). Ryanodine was obtained from Calbiochem. B[*a*]P-7,8-diol, (±)anti-BPDE, epoxide, and diones were obtained from the National Cancer Institute's Chemical Repository at the Midwestern Research Institute (Kansas City, MO), except for the B[*a*]P-7,8-dione, which was synthesized according to published methods (Sukumuran and Harvey, 1980). All PAHs were assessed for purity by high-performance liquid chromatography and were greater than 95% pure at the time of use. Stock (1000×) PAH were prepared in anhydrous DMSO and were stored at −80°C under nitrogen until used.

Results

B[*a*]P-7,8-dione Selectively Mobilizes Ca^{2+} from SR. Ca^{2+} fluxes were measured across SR vesicles under conditions of active loading in the presence of ATP and a regenerating system. Once Ca^{2+} loading approached 70 to 80% of the empirically determined capacity of the vesicles, B[*a*]P and its metabolites (Fig. 1) were added singly to test their ability to release accumulated Ca^{2+}. B[*a*]P-7,8-dione was found to have a high efficacy toward mobilizing stored Ca^{2+}, giving an efflux rate of 2.2 μmol Ca^{2+} mg^{-1} min^{-1} (Fig. 2). By contrast, B[*a*]P, B[*a*]P-3,6-dione, B[*a*]P-6,12-dione, B[*a*]P-7,8-diol, and (±)-*anti*-BPDE failed to mobilize Ca^{2+} from actively loaded SR vesicles under the assay conditions used.

The activity exhibited by B[*a*]P-7,8-dione could be the result of 1) inhibition of SERCA pump activity, 2) activation of the Ca^{2+} release channel RyR1, 3) nonspecific membrane effects, or 4) a combination of these mechanisms. To test among these possibilities, SR was sequentially loaded with Ca^{2+} and B[*a*]P-7,8-dione was introduced into the cuvette once the loading phase was complete (Fig. 3, top trace). Once B[*a*]P-7,8-dione released all the stored Ca^{2+}, 2 μM ruthenium red (RR), a known blocker of RyR1, was introduced into the transport medium. Blockade of RyR1 by RR resulted in the complete reaccumulation of Ca^{2+} into SR vesicles. In previous studies, a high concentration of ryanodine was shown to initially activate then inhibit RyR1, thereby producing a sequential efflux then reuptake of Ca^{2+} into SR vesicles under conditions of active loading (Pessah and Zimanyi, 1991). B[*a*]P-7,8-dione was ineffective at mobilizing Ca^{2+} when added to the reaction cuvette after ryanodine blocked RyR1 channels (Fig. 3, second trace). Finally, addition of B[*a*]P-7,8-dione to Ca^{2+}-loaded vesicles shortly after RR also failed to induce release (Fig. 3, third trace). These results revealed B[*a*]P-7,8-dione to be the only PAH metabolite to induce the release of Ca^{2+} from SR by a selective mechanism that appears to involve RyR1.

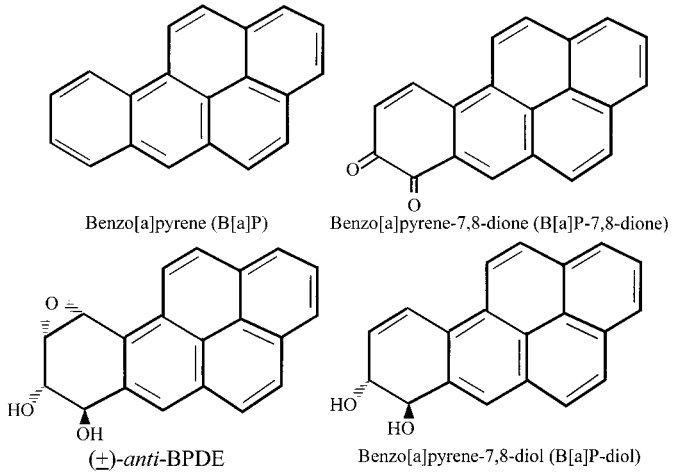

Fig. 1. Structures of benzo[*a*]pyrene and relevant metabolites.

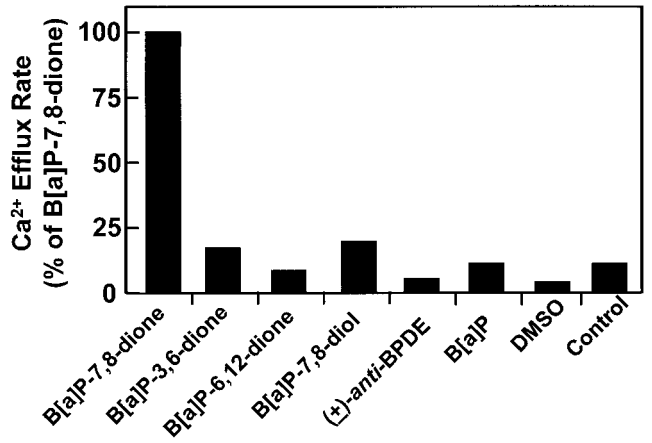

Fig. 2. Among related B[*a*]P structures, only B[*a*]P-7,8-dione induces net Ca^{2+} efflux from actively loaded junctional sarcoplasmic reticulum. Ca^{2+} fluxes were measured with antipyrylazo III in cuvettes containing 40 μg/ml of microsomal protein in transport buffer consisting of MgATP (1 mM) and coupling enzyme as described under *Materials and Methods*. Vesicles were actively loaded by seven sequential additions of $CaCl_2$ (20 μM). Upon completion of the loading phase, B[*a*]P-7,8-dione, B[*a*]P-3,6-dione, B[*a*]P-6,12-dione, B[*a*]P-7,8-diol, (±)-*anti*-BPDE, B[*a*]P (each at a final concentration of 10 μM), or DMSO (10 μL) were added and the change in extravesicular Ca^{2+} monitored at 710 to 790 nm. The rate giving 100% was 2.17 μmol of Ca^{2+} mg^{-1} min^{-1}. The data is the average of two determinations.

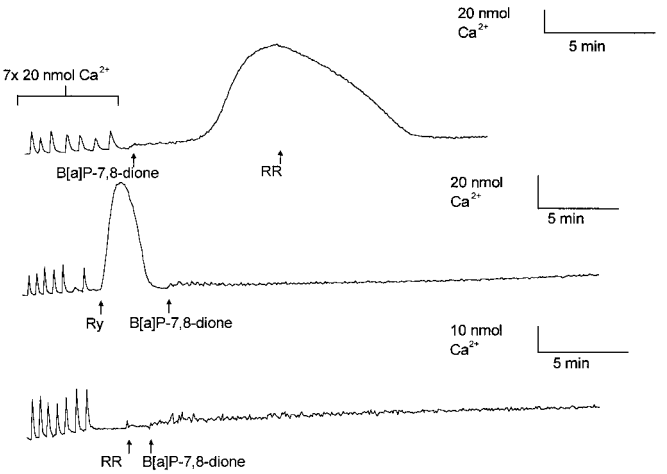

Fig. 3. B[*a*]P-7,8-dione induces microsomal Ca^{2+} release by selective activation of ryanodine receptor type 1 (RyR1). Cuvettes containing microsomal vesicles (40 μg/ml protein) in Ca^{2+} transport buffer were actively loaded by seven sequential additions of $CaCl_2$ (20 μM each). Top trace, when loading was complete, a saturating concentration of B[*a*]P-7,8-dione (10 μM) was introduced into the cuvette (first arrow). RR (2 μM), a selective blocker of RyR1, was added at the peak of the B[*a*]P-7,8-dione response (second arrow), and the vesicles actively reaccumulated the released Ca^{2+}. Middle trace, when loading was complete, the alkaloid ryanodine (Ry; 500 μM) was introduced to the reaction mixture (first arrow), causing a characteristic sequential activation and irreversible inhibition of RyR1. After the RyRs were blocked, an addition of B[*a*]P-7,8-dione (10 μM) was unable to induce release of the accumulated intravesicular Ca^{2+} (second arrow). Bottom trace, when the Ca^{2+} loading phase was completed, RR (2 μM) was first introduced (first arrow). Approximately 1 min later, B[*a*]P-7,8-dione (10 μM) was added (second arrow) although it was ineffectual in releasing microsomal Ca^{2+}. The effects of B[*a*]P-7,8-dione were consistently inhibited by known blockers/inactivators of RyR. Each experiment was repeated at least three times with similar results.

Because RyR1 and related isoforms constitute CICR channels, we examined the Ca^{2+}-dependence of B[a]P-7,8-dione-induced Ca^{2+} release. The potency and efficacy of B[a]P-7,8-dione to induce Ca^{2+} release was highly dependent on extravesicular Ca^{2+}. In the presence of 5 μM extravesicular Ca^{2+}, B[a]P-7,8-dione enhanced CICR in a dose-dependent manner with a threshold of 400 nM and an EC_{50} value of 2 μM. The maximum release rate was nearly 2 μmol of Ca^{2+} mg^{-1} min^{-1} (Fig. 4A&B). By contrast, in the presence of 100 nM extravesicular Ca^{2+}, the threshold and EC_{50} values obtained for B[a]P-7,8-dione-induced Ca^{2+} release were 5- and 3-fold higher (2 and 6 μM), respectively, than those measured at higher extravesicular Ca^{2+}. The maximum rate of Ca^{2+} release attained with B[a]P-7,8-dione in the presence of 100 nM extravesicular Ca^{2+} was nearly 15-fold smaller compared with the rate seen in the presence of 5 μM extravesicular Ca^{2+}. The onset of Ca^{2+} release induced by B[a]P-7,8-dione exhibited a characteristic delay (Fig. 3) from the time it was added to the vesicles. We therefore studied the relationship between concentration and the time necessary to release 15% of the total accumulated Ca^{2+} (Fig. 5). In this regard, the time required to release 15% of the accumulated Ca^{2+} was inversely related to B[a]P-7,8-dione concentration.

Earlier studies indicated that SERCA pump inhibition might account for altered Ca^{2+} regulation observed in cells with PAHs (Krieger et al., 1995). More recently, PAHs examined for their effects on purified cloned rat SERCA enzymes failed to show inhibitory potency, suggesting that PAH metabolites such as quinones might be inhibitors of SERCA pumps and might be the proximate agents that disrupt Ca^{2+} homeostasis in cells (Zhao et al., 1996). We tested this hypothesis directly by measuring Ca^{2+}-dependent ATPase activity in the presence and absence B[a]P or B[a]P-7,8-dione. The junctional SR membranes used in these studies contained >95% Ca^{2+}-dependent ATPase and this activity was fully inhibited by thapsigargin. B[a]P at a concentration as high as 20 μM failed to inhibit SERCA activity (not shown). Likewise, B[a]P-7,8-dione $\leq$15 μM did not inhibit SERCA activity; the rates of ATP hydrolysis were not different from paired DMSO controls (Fig. 6). Taken together, these results reveal that although B[a]P-7,8-dione is an efficacious enhancer of microsomal Ca^{2+} release, its activity is not mediated through SERCA inhibition.

B[a]P-7,8-dione Induces Direct Biphasic Actions on RyR1 Function. Recently it has been shown that nanomolar concentrations of redox-active naphthalene-1,4-dione enhance SR Ca^{2+} release by modifying RyR1 activity, whereas low micromolar concentrations produce a time-dependent activation and subsequent inhibition of RyR1 function (Feng et al., 1999). We examined whether a direct modification of RyR1 function could account for B[a]P-7,8-dione-induced changes in microsomal Ca^{2+} fluxes described above. Single RyR1 channels were reconstituted in bilayer lipid membranes and the influence of B[a]P-7,8-dione on channel gating kinetics studied under voltage clamp. Figure 7A shows

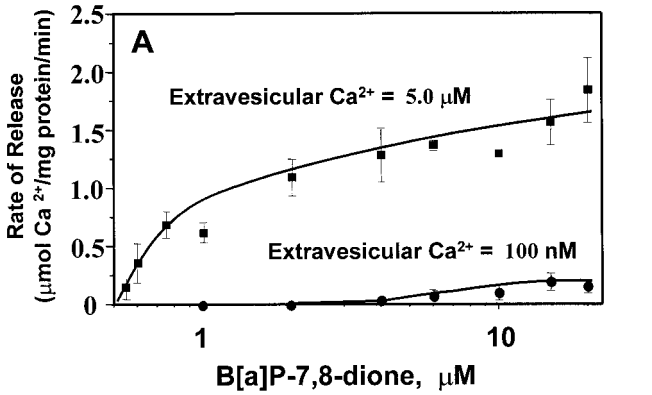

Fig. 4. B[a]P-7,8-dione induces microsomal Ca^{2+} release in a dose- and Ca^{2+}-dependent manner. Vesicles (40 μg/ml protein) were actively loaded by seven sequential additions of $CaCl_2$ (20 μM each). After the active loading phase, B[a]P-7,8-dione was added to the cuvette. Rates were taken as the difference between the B[a]P-7,8-dione-containing reaction vessel and a control reaction vessel, which was measured in parallel. A, dose responses were performed either in the presence of 100 nM (●) or 5 μM (■) free extravesicular Ca^{2+}. Data shown are the average and range of two trials (■) or the mean and S.D. of three trials (●). Ionophore A23187 was added at the end of each experiment to assure equal loading and to calibrate the dye signal. B, dose-response data were analyzed by logit-log plots. Linear regression was performed to determine the slope and EC_{50} value. The presence of 5 μM free extravesicular Ca^{2+} (■), a concentration that sensitizes RyR1 to CICR, produced a threshold and EC_{50} value for 7,8 BPQ of 400 nM and 2 μM, respectively. The logit slope was 0.82. By contrast, in the presence of 100 nM extravesicular Ca^{2+} (●), a concentration that minimizes CICR, gave a threshold and EC_{50} value of 2 μM and 6 μM, respectively. The logit slope was 2.0. The maximum rates of release with saturating B[a]P-7,8-dione were 1.92 and 0.12 μmol Ca^{2+} mg^{-1} min^{-1} in the presence of 5 μM and 100 nM free extravesicular Ca^{2+}, respectively, a difference in efficacy of 16-fold.

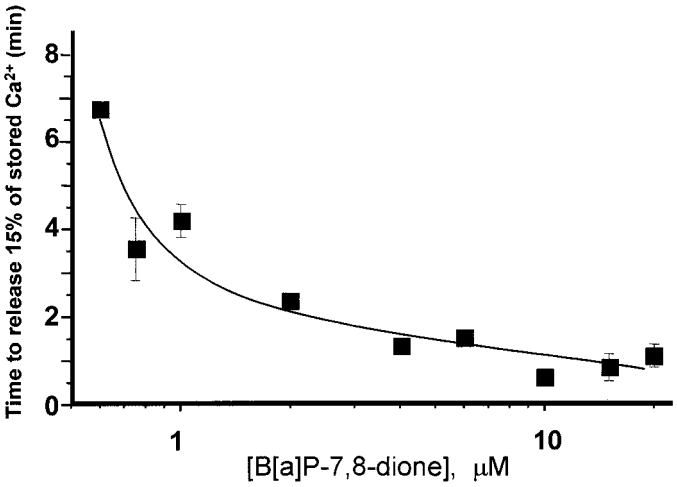

Fig. 5. B[a]P-7,8-dione mobilizes microsomal Ca^{2+} in a time-dependent manner. Cuvettes containing microsomal vesicles (40 μg/ml protein) were actively loaded by seven sequential additions of $CaCl_2$ (20 μM each). Following active loading, B[a]P-7,8-dione was added to the cuvette in the presence of 5 μM final free Ca^{2+}. The time to release ~15% (20 nmol) of the total stored Ca^{2+} (140 nmol) was measured as a function of B[a]P-7,8-dione concentration. The data shown are mean ± S.D. of three determinations.

the gating kinetics of a typical RyR1 channel in the presence of 7 μM Ca^{2+} on the cytoplasmic (*cis*) side of the bilayer lipid membrane chamber. Under these conditions, channel transitions from closed to open are extremely fast, but rare, giving an open probability (P_o) of 0.011. After addition of 1 μM B[*a*]P-7,8-dione to the *cis* chamber, the P_o increased 7-fold to 0.079. However, within 10 min of introducing B[*a*]P-7,8-dione, the channel ceased to gate. Figure 7B shows the same type of experiment performed on another channel with higher (100 μM) Ca^{2+} in the *cis* chamber. Although the channel initially has a higher P_o because of the optimal *cis* Ca^{2+} for channel activation, addition of 1 μM B[*a*]P-7,8-dione enhanced P_o by approximately 6-fold. As seen with lower *cis* Ca^{2+}, the activating effect of B[*a*]P-7,8-dione was transient, culminating in persistent inhibition of the channel within 10 min. Figure 7C shows 12 min of continuous channel recording, highlighting the biphasic actions of B[*a*]P-7,8-dione on RyR1. In separate experiments, addition of B[*a*]P to 10 μM failed to alter channel activity over a period of 10 min (not shown).

The biphasic, time-dependent actions of B[*a*]P-7,8-dione were independently verified by measuring active Ca^{2+} accumulation by SR vesicles. SR exposed 1 μM B[*a*]P-7,8-dione 10 min before initiating active Ca^{2+} loading exhibited a significant reduction in the initial rate of Ca^{2+} accumulation compared with solvent control. By contrast, 20 μM B[*a*]P-7,8-dione tested under the same experimental conditions resulted in a significant increase in the rate of Ca^{2+} accumulation (data not shown).

The activating actions of B[*a*]P-7,8-dione could also be demonstrated using radioligand receptor binding analysis with [^{3}H]ryanodine. [^{3}H]Ryanodine binds to RyR1 with nanomolar affinity when the channel is in the open state (Pessah et al., 1987). The rate of receptor occupancy by [^{3}H]ryanodine therefore provides a biochemical measure of channel P_o. Table 1 reveals that 100 nM B[*a*]P-7,8-dione enhances the apparent association rate 2-fold, whereas 1 μM B[*a*]P-7,8-dione enhanced the rate 6-fold, in good agreement with results from the bilayer lipid membrane. However, the level of receptor occupancy at the *pseudo* steady-state plateau is progressively lower in the presence of 0.1 and 1 μM B[*a*]P-7,8-dione, indicating that although channel P_o is enhanced by the *o*-quinone, the number of functional channels declines with time. These results provide independent evidence for the biphasic nature by which B[*a*]P-7,8-dione modifies RyR1 channel function.

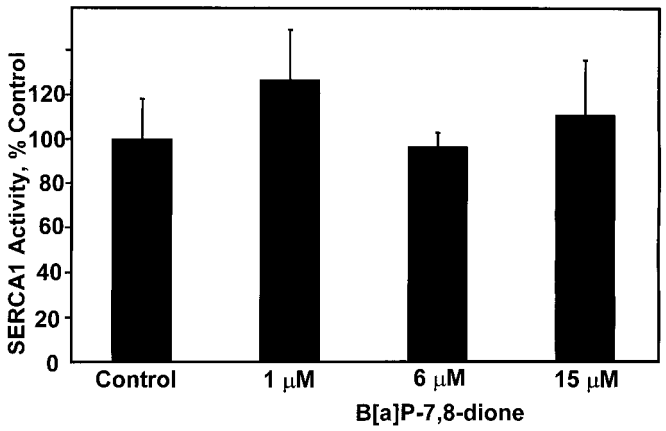

Fig. 6. B[*a*]P-7,8-dione does not significantly alter the rate of Ca^{2+}-dependent ATP hydrolysis by SERCA pumps at concentrations that maximally stimulate RyR1. Microsomes (10.4 μg/ml protein) were added to an ATPase buffer containing coupling enzymes, substrates, NADH, and Ca^{2+} ionophore as defined under *Materials and Methods*. Ca^{2+}-dependent oxidation of NADH was monitored at 340 nm. After 1-min equilibration, Na_2ATP (1 mM) was added to the reaction to commence measurement of total ATPase activity. After 3 min, EGTA (4 mM) was added to determine the Ca^{2+}-independent rate of ATP hydrolysis. Rate of ATP hydrolysis by SERCA pump was reported as the difference between total and Ca^{2+} independent rates of hydrolysis. In these microsomal preparations, SERCA activity accounted for ≥95% of the total ATPase activity. Each condition was repeated at least twice and the bar graph reports the mean value with the corresponding S.D.

Discussion

Polycyclic aromatic hydrocarbons are environmental pollutants that are known to be carcinogenic and immunotoxic. In intact cell assays, B[*a*]P in particular has been shown to disrupt Ca^{2+} homeostasis in both immune and nonimmune

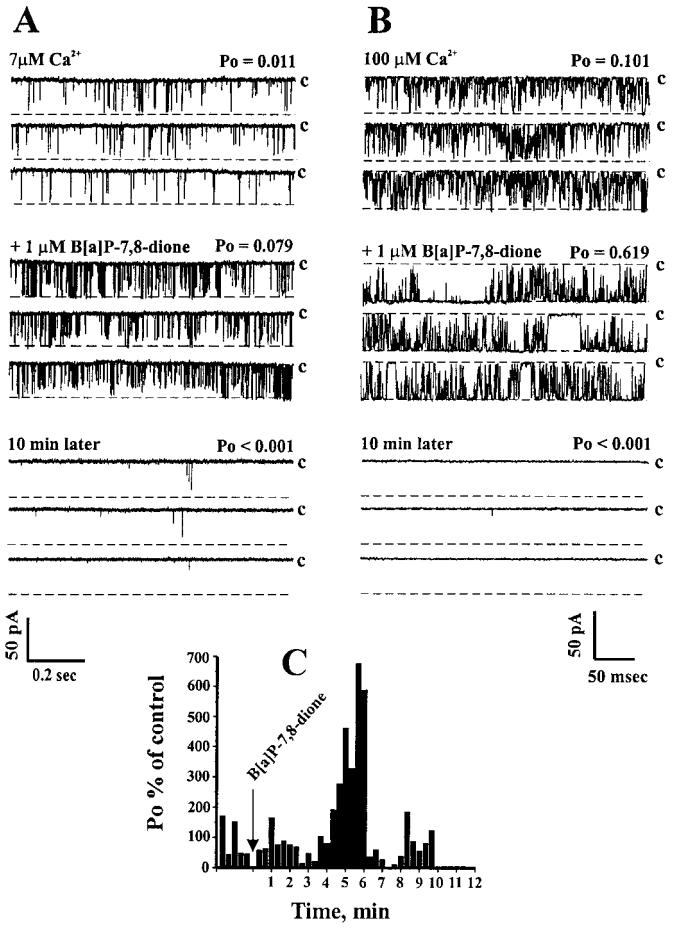

Fig. 7. B[*a*]P-7,8-dione modifies RyR1 channel gating kinetics in a biphasic manner. Single RyR1 channels were reconstituted in planar bilayer lipid membranes and current transitions measured under voltage clamp as described under *Materials and Methods*. A, a typical channel exhibiting low P_o in the presence of suboptimal cytoplasmic Ca^{2+} (7 μM). After addition of 1 μM B[*a*]P-7,8-dione to the cytoplasmic side of the channel, transiently increased P_o by 7-fold. Within 10 min of addition, B[*a*]P-7,8-dione induced channel closure. B, a typical channel in the presence of optimal cytoplasmic Ca^{2+} exhibits higher P_o (more frequent transitions to the open state). Addition of B[*a*]P-7,8-dione to the cytoplasmic side of the channel further increases P_o 6-fold; again, this activation is transient. Within 10 min, B[*a*]P-7,8-dione induces channel closure. C, a summary showing the fluctuation of channel P_o from a complete 12-min record. Note the characteristic delay in the onset of B[*a*]P-7,8-dione-induced channel activation and subsequent inhibition. These results were repeated on four separate channels.

TABLE 1.
B[a]P-7,8-dione modulates the binding kinetics of [^{3}H]ryanodine to RyR1 in a concentration-dependent manner.

	Control	B[a]P-7,8-dione, 0.1 μM	B[a]P-7,8-dione, 1 μM
k_{obs}(min^{-1})	0.0314 ± 0.0014	0.0642 ± 0.0134	0.193 ± 0.018
$T_{1/2}$ (min)	22.1 ± 0.9	11.1 ± 2.2	3.6 ± 0.3
B_{eq} (pmol/mg)[a]a	2.81 ± 0.24	2.20 ± 0.28	1.48 ± 0.04

[a]a [^{3}H]Ryanodine occupancy at steady state
k_{obs}, observed association rate constant; $T_{1/2}$, half-time to steady state.

cells, but the molecular mechanism has not been defined. Using a well-defined junctional SR model system, the present study identifies for the first time that a single *o*-quinone metabolite of B[*a*]P, B[*a*]P-7,8-dione, can account for altered Ca^{2+} transport across the microsomal membrane. The key findings in this study are: 1) metabolic bioactivation of B[*a*]P to B[*a*]P-7,8-dione is required for deregulation of Ca^{2+} transport. Other metabolites, including the B[*a*]P-3,6- and -6,12-diones, the B[*a*]P-7,8-diol, and the (±)-*anti*-BPDE, lack activity at the concentrations tested. 2) B[*a*]P-7,8-dione disrupts Ca^{2+} transport by influencing the activity of RYR1 without any measurable influence on SERCA or membrane integrity. 3) The actions of B[*a*]P-7,8-dione are biphasic, involving a time-dependent activation and subsequent inactivation of channel function.

Several different reactive metabolites of B[*a*]P are derived from P450-dependent pathways. The P450 pathways represented by CYP1A1 or CYP1B1 form phenolic metabolites and epoxides and, in the presence of epoxide hydrolase, produce the 7,8-dihydrodiol of B[*a*]P (B[*a*]P-7,8-diol). B[*a*]P-7,8-diol can enter another round of metabolism by CYP1A1 or CYP1B1 to form 7,8-diol-9,10-epoxide of B[*a*]P [(±)-*anti*-BPDE] (Conney, 1982). In addition to the metabolism of diols and diol-epoxides, cytochrome P450 enzymes can also catalyze the production of hydroxylated metabolites leading to the B[*a*]P-6,12-, 1,6-, and 3,6-diones. The cytochrome P450-peroxidase activity will also give rise to reactive radical cations (Cavalieri and Rogan, 1995). Recent studies have shown that *o*-quinones can also be formed from the B[*a*]P-7,8-diol in the presence of dihydrodiol dehydrogenase, members of the aldo-ketoreductase (AKR) superfamily (Smithgall et al., 1988; Penning et al., 1999). B[*a*]P *o*-quinones are of interest because they undergo redox-cycling, leading to the production of oxygen free radicals that can exert oxidative stress in cells. Within this metabolic scheme, enzymatic oxidation of B[*a*]P-diol leads to the formation of a catechol that undergoes autoxidation to form B[*a*]P-7,8-dione. Conversion to the *o*-quinone results in production of reactive oxygen species. Once formed, the *o*-quinone can either enter futile redox cycles to generate reactive oxygen species or it can form thioether conjugates. In support of one or more "bioactivation" steps in B[*a*]P-induced Ca^{2+} mobilization from microsomal stores, Burchiel and coworkers have shown that certain oxidative and electrophilic metabolites of B[*a*]P increase intracellular Ca^{2+} in human B cells (Mounho and Burchiel, 1998) and human mammary epithelial cells (Tannheimer et al., 1999). Dimunition of B[*a*]P-induced increases in intracellular Ca^{2+} by the AhR partial antagonist and cytochrome P450 inhibitor, α-naphthaflavone, suggests that cytochrome P450 metabolism is required for altered Ca^{2+} homeostasis in lymphoid and nonlymphoid cells. Elevation of intracellular Ca^{2+} may be associated with altered cell proliferation in human mammary epithelial cells (Tannheimer et al., 1997) and the induction of apoptosis in human B cells (Salas and Burchiel, 1998).

It is not easy to assess which tissues may be affected by B[*a*]P-7,8-dione. Five different human AKRs are responsible for its formation from the corresponding BP-7,8-diol. These are AKR1C1 through AKR1C4 and AKR1A1 (which is aldehyde reductase) (Burczynski et al., 1998). Tissue distribution studies show that AKR1C4 is hepatic specific, whereas the remaining isoforms each show their own patterns of distribution and differ in their catalytic efficiencies for BP-7,8-diol (Penning et al., 2000). Liver has been shown to possess specific [^{3}H]ryanodine-binding protein (Shoshan-Barmatz et al., 1991). Moreover, breast cancer cells (MCF10A) and such immune cells as B-lymphocytes, also suspected targets of B[*a*]P and its metabolites, have been shown to express RyR (S. W. Burchiel and I. N. Pessah, unpublished observations). However, further confounding this issue is whether these isoforms are coexpressed with CYP1A1 and epoxide hydrolase, which are required for the production of the diol substrate. Also, of these human isozymes, AKR1C1 can be robustly induced by planar aromatics and reactive oxygen (Burczynski et al., 1999).

Within the metabolic scheme involving AKRs, B[*a*]P-7,8-dione is the only compound that exhibits potent and efficacious disruption of microsomal Ca^{2+} transport. Furthermore toxicologically relevant concentrations (nanomolar to low micromolar) of B[*a*]P-7,8-dione alter Ca^{2+} transport by a highly selective mechanism involving RYR1 without measurable changes in SR membrane integrity or decreased SERCA pump activity. Considering the emerging role of hyper-reactive sulfhydryl chemistry in regulating RyR complexes (Pessah and Feng, 2000), this finding is not surprising. A small number of hyper-reactive thiols have been shown to exist within the RyR complex (Liu et al., 1994; Liu and Pessah, 1994). Their functional role does not seem to directly affect overt aspects of channel gating. Rather hyper-reactive Cys moieties may represent biochemical components of a redox sensor that conveys information about localized changes in redox potential produced by physiologic (e.g., glutathione, nitric oxide) and pathophysiologic (e.g., quinones, reactive oxygen species) channel modulators to the Ca^{2+} release process.

Recently, the functional role of hyper-reactive sulfhydryl moieties within the RyR complex in Ca^{2+} deregulation by redox active quinones such as naphthalene-1,4-dione (Feng et al., 1999). 7-Diethylamino-3-(4′-maleimidylphenyl)-4-methylcoumarin (CPM, a fluorogenic maleimide) was used to measure the reactivity of hyper-reactive sulfhydryl moieties on SR membranes in the presence and absence of naphthalene-1,4-dione by analyzing the kinetics of forming CPM-thioether adducts and localization of fluorescence by SDS-PAGE. Naphthalene-1,4-dione (NQ) selectively and dose dependently (EC_{50} = 0.3 μM) interacts with a class of hyper-reactive sulfhydryl groups local-

ized on RyR1 and its associated protein triadin. Similar to B[*a*]P-7,8-dione in the present study, nanomolar NQ enhanced the association of [^{3}H]ryanodine for its high-affinity binding site and directly enhanced channel P_o in bilayer lipid membrane measurements in a reversible manner. By contrast, micromolar NQ produced a time-dependent biphasic action on channel function, leading to irreversible channel inactivation. Most importantly, the sensitivity to redox-active quinones was eliminated upon formation of thioether adducts between CPM and the most reactive thiols of the RyR channel complex. The Ca^{2+}-dependent cytotoxicities observed with reactive quinones formed at the microsomal surface by oxidative metabolism may be related to their ability to selectively modify hyper-reactive thiols regulating normal functioning of microsomal Ca^{2+} release channels. Importantly, these results raise the possibility that microsomal Ca^{2+} channels may actually utilize hyper-reactive sulfhydryl chemistry in "sensing" localized changes in redox environment. B[*a*]P-7,8-dione undergoes 1,4-Michael addition with thiols to yield catechol conjugates which then autooxidize to give *o*-quinone thiol-ether conjugates with the production of reactive oxygen species (Smithgall et al., 1988). In addition, measurements of oxygen metabolism during the AKR-dependent oxidation of B[*a*]P-7,8-diol to B[*a*]P-7,8-dione showed that hydrogen peroxide was formed before undergoing arylation reactions with GSH or protein acceptors. Thus the biphasic effects observed with B[*a*]P-7,8-dione could be explained by its redox and electrophilic properties. The early activation phase could be the direct result of redox cycling with hyper-reactive (redox sensing) Cys within the RyR1 complex, whereas the subsequent inhibition phase may result from arylation of the receptor at one or more sites. Importantly hydrogen peroxide has been shown to activate RyR1 and microsomal Ca^{2+} release (Favero et al., 1995). Exposure of intact cells to B[*a*]P could also influence redox sensing indirectly by local production of hydrogen peroxide and/or changes in the ratio of GSH to GSSG (Zable et al., 1997; Feng et al., 2000), provided the appropriate oxidative and AKR1C enzymes are expressed. What drives redox cycling in these in vitro measurements that lack any exogenously added reducing equivalents (e.g., NADPH, GSH)? One possible mechanism is that the primary electron donor is the RyR1 complex itself. Alternatively, Michael addition of either thiols or buffer nucleophiles to the quinone will produce a ketol, which will rearrange to a catechol conjugate. The catechol conjugate will autoxidize in air to produce reactive oxygen species on route to the *o*-semiquinone anion radical and eventually the quinone conjugate. If contaminating transition metal ions were present, they would catalyze the 1-electron redox-cycle between the *o*-semiquinone anion radical and the catechol conjugate with concomitant production of reactive oxygen (Flowers et al., 1997). This situation will exist unless all solutions used in the assay were Chelex treated.

In conclusion, RyR1 and its two alternate isoforms are broadly expressed in mammalian cell types. For example, RyR1 has been recently identified in B lymphocytes (Sei et al., 1999) and RyR protein is expressed MCF10A breast cancer cells (I. N. Pessah and S. W. Burchiel, unpublished observations). Considering the important role of RyR in Ca^{2+}-signaling, the observation of a selective mechanism mediating RyR dysfunction by B[*a*]P-7,8-dione may be of pathophysiological significance.

References

Archuleta MM, Schieven GL, Ledbetter JA, Deanin GG and Burchiel SW (1993) 7,12-Dimethylbenz[a]anthracene activates protein-tyrosine kinases Fyn and Lck in the HPB-ALL human T-cell line and increases tyrosine phosphorylation of phospholipase C-gamma 1, formation of inositol 1,4,5-trisphosphate, and mobilization of intracellular calcium. *Proc Natl Acad Sci USA* **90:**6105–6109.

Baum EJ (1978) Occurrence and surveillance of polycyclic aromatic hydrocarbons. In: *Polycyclic Hydrocarbons and Cancer, Environment Chemistry, and Metabolism* (Gelboin HV and Ts'O POP eds), p. 45, Academic Press, New York.

Burczynski ME, Harvey RG and Penning TM (1998) Expression and characterization of four recombinant human dihydrodiol dehydrogenase isoforms: Oxidation of *trans*-7,8-dihydroxy-7,8-dihydrobenzo[a]pyrene to the activated *o*-quinone metabolite benzo[a]pyrene-7,8-dione. *Biochemistry* **37:**6781–90.

Burczynski ME, Lin HK and Penning TM (1999) Isoform-specific induction of a human aldo-keto reductase by polycyclic aromatic hydrocarbons (PAHs), electrophiles, and oxidative stress: Implications for the alternative pathway of PAH activation catalyzed by human dihydrodiol dehydrogenase. *Cancer Res* **59:**607–614.

Cavalieri EL and Rogan EG (1995) Central role of radical cations in metabolic activation of polycyclic aromatic hydrocarbons. *Xenobiotica* **25:**677–688.

Conney AH (1982) Induction of microsomal enzymes by foreign chemicals and carcinogens by polycyclic aromatic hydrocarbons; G.H.A. Clowes Memorial Lecture. *Cancer Res* **42:**4875–4917.

Davila DR, Romero DL and Burchiel SW (1996) Human T cells are highly sensitive to suppression of mitogenesis by polycyclic aromatic hydrocarbons and this effect is differentially reversed by α-naphthoflavone. *Toxicol Appl Pharmacol* **139:**333–341.

Davila DR, Lane JL, Lauer FT and Burchiel SW (1999) Nonspecific factors influence protein tyrosine kinase activation by polycyclic aromatic hydrocarbons in human HPB-ALL T cells. *J Toxicol Env Health* **56:**101–113.

Dipple A (1994) Reactions of polycyclic aromatic hydrocarbons with DNA. *IARC Sci Publ* **125:**107–129.

Ethier SP and Ullrich RL (1982) Detection of ductal dysplasia in mammary outgrowths derived from carcinogen-treated virgin female BALB/C mice. *Cancer Res* **42:**1753–1760.

Fabiani R, De Bartolomeo A, Rosignoli P, Sebastiani B and Morozzi G (1999) Priming effect of benzo[a]pyrene on monocyte oxidative metabolism: Possible mechanisms. *Toxicol Lett* **110:**11–18.

Favero TG, Zable AC and Abramson JJ (1995) Hydrogen peroxide stimulates the Ca^{2+} release channel from skeletal muscle sarcoplasmic reticulum. *J Biol Chem* **270:**25557–25563.

Feng W, Liu G, Xia R, Abramson JJ and Pessah IN (1999) Site-selective modification of hyperreactive cysteines of ryanodine receptor complex by quinones. *Mol Pharmacol* **55:**821–831.

Feng W, Liu G, Allen PD and Pessah IN (2000) Transmembrane redox sensor of ryanodine receptor type 1 (RyR1). *J Biol Chem* **275:**35902–35907.

Flowers-Geary L, Harvey RG and Penning TM (1993) Cytotoxicity of polycyclic aromatic hydrocarbon *o*-quinones in rat and human hepatoma cells *Chem Res Toxicol* **6:**252–260.

Flowers-Geary L, Harvey RG and Penning TM (1995) Identification of benzo-[a]pyrene-7,8-dione as an authentic metabolite of (±)-*trans*-7,8-dihydroxy-7,8-dihydrobenzo[a]pyrene in isolated rat hepatocytes. *Carcinogenesis* **16:**2707–2715.

Flowers-Geary L, Beczinski W, Harvey RG and Penning TM (1996) Cytotoxicity and mutagenicity of polycyclic aromatic hydrocarbon o-quinones produced by dihydrodiol dehydrogenase. *Chem-Biol Interact* **99:**55–72.

Flowers L, Ohnishi ST and Penning TM (1997) DNA strand scission by polycyclic aromatic hydrocarbon o-quinones: Role of reactive oxygen species, Cu(II)/Cu(I) redox cycling, and o-semiquinone anion radicals. *Biochemistry* **36:**8640–8648.

Holsapple MP, Karras JG, Ledbetter JA, Schieven GL, Burchiel SW, Davila DR, Schatz AR and Kaminski NE (1996) Molecular mechanisms of toxicant-induced immunosuppression: Role of second messengers. *Annu Rev Pharmacol Toxicol* **36:**131–159.

Krieger JA, Davila DR, Lytton J, Born JL and Burchiel SW (1995) Inhibition of sarcoplasmic/endoplasmic reticulum calcium ATPases (SERCA) by polycyclic aromatic hydrocarbons in HPB-ALL human T cells and other tissues. *Toxicol Appl Pharmacol* **133:**102–108.

Liu G and Pessah IN (1994) Molecular interaction between ryanodine receptor and glycoprotein triadin involves redox cycling of functionally important hyperreactive sulfhydryls. *J Biol Chem* **269:**33028–33034.

Liu G, Abramson JJ, Zable AC and Pessah IN (1994) Direct evidence for existence and functional role of hyperreactive sulfhydryls on ryanodine receptor-triadin complex selectively labeled by the coumarin maleimide 7-dimethylamino-3-(4′-maleimidylphenyl)-4-methylcoumarin. *Mol Pharmacol* **45:**189–200.

Mounho BJ and Burchiel SW (1998) Alterations in human B cell calcium homeostasis by polycyclic aromatic hydrocarbons: Possible associations with cytochrome P450 metabolism and increased protein tyrosine kinase phosphorylation. *Toxicol Appl Pharmacol* **149:**80–89.

Mounho BJ, Davila DR and Burchiel SW (1997) Characterization of intracellular calcium responses produced by polycyclic aromatic hydrocarbons in surface marker-defined human peripheral blood mononuclear cells. *Toxicol Appl Pharmacol* **145:**323–330.

Palade P (1987) Drug-induced Ca^{2+} release from isolated sarcoplasmic reticulum. I. Use of pyrophosphate to study caffeine-induced Ca^{2+} release. *J Biol Chem* **262:**6135–6141.

Penning TM, Burczynski ME, Jez JM, Hung C-F, Lin H-K, Ma H, Moore M, Palackal N and Rathnam K (2000) Human 3-hydroxysteroid dehydrogenase isoforms (AKR1C1–AKR1C4) of the aldo-keto reductase superfamily: Functional plasticity and tissue distribution reveals roles in the inactivation and formation of male and female sex hormones. *Biochem J* **351:**67–77.

Penning TM, Burczynski ME, Hung CF, McCoull KD, Palackal NT and Tsuruda LS (1999) Dihydrodiol dehydrogenases and polycyclic aromatic hydrocarbon activation: Generation of reactive and redox active *o*-quinones. *Chem Res Toxicol* **12:**1–18.

Pessah IN and Feng W (2000) Functional role of hyperreactive sulfhydryl moieties within the ryanodine receptor complex. *Antioxidants & Redox Signaling* **2:**17–25.
Pessah IN, Stambuk RA and Casida JE (1987) Ca^{2+}-activated ryanodine binding: Mechanism of sensitivity and intensity modulation by Mg^{2+}, caffeine, and adenine nucleotides. *Mol Pharmacol* **31:**232–238.
Pessah IN and Zimanyi I (1991) Characterization of multiple [^{3}H]ryanodine-binding sites on the Ca^{2+} release channel of sarcoplasmic reticulum from skeletal and cardiac muscle: Evidence for a sequential mechanism in ryanodine action. *Mol Pharmacol* **39:**679–689.
Romero DL, Mounho BJ, Lauer FT, Born JL and Burchiel SW (1997) Depletion of glutathione by benzo(a)pyrene metabolites, ionomycin, thapsigargin, and phorbol myristate in human peripheral blood mononuclear cells. *Toxicol Appl Pharmacol* **144:**62–69.
Saito A, Seiler S, Chu A and Fleischer S (1984) Preparation and morphology of sarcoplasmic reticulum terminal cisternae from rabbit skeletal muscle. *J Cell Biol* **99:**875–885.
Salas VM and Burchiel SW (1998) Apoptosis in Daudi human B cells in response to benzo[a]pyrene and benzo[a]pyrene-7,8-dihydrodiol. *Toxicol Appl Pharmacol* **151:** 367–376.
Schwartz A, Allen JC and Harigaya S (1969) Possible involvement of cardiac Na^+, K^+-adenosine triphosphatase in the mechanism of action of cardiac glycosides. *J Pharmacol Exp Ther* **168:**31–41.
Sei Y, Gallagher KL and Basile AS (1999) Skeletal muscle type ryanodine receptor is involved in calcium signaling in human B lymphocytes. *J Biol Chem* **274:**5995–6002.
Shoshan-Barmatz V, Pressley TA, Higham S and Kraus-Friedmann N (1991) Characterization of high-affinity ryanodine-binding sites of rat liver endoplasmic reticulum. Differences between liver and skeletal muscle. *Biochem J* **276:**41–46.
Smithgall TE, Harvey RG and Penning TM (1988) Spectroscopic identification of ortho-quinones as the products of polycyclic aromatic *trans*-dihydrodiol oxidation catalyzed by di-hydrodiol dehydrogenase. *J Biol Chem* **263:**1814–1820.
Sukumuran KB and Harvey RG (1980) Synthesis of o-quinones and dihydrodiols of polycyclic aromatic hydrocarbons from the corresponding phenols. *J Org Chem* **45:**4407–4413.
Tannheimer SL, Ethier SP and Burchiel SW (1997) Carcinogenic polycyclic aromatic hydrocarbons increase intracellular Ca^{2+} in primary human mammary epithelial cells. *Carcinogenesis* **18:**1177–1182.
Tannheimer SL, Ethier SP, Caldwell KK and Burchiel SW (1998) Polycyclic aromatic hydrocarbon-induced alterations in tyrosine phosphorylation and insulin-like growth factor signaling pathways in the MCF-10A human mammary epithelial cell line. *Carcinogenesis* **19:**1291–1297.
Tannheimer SL, Lauer FT, Lane JL and Burchiel SW (1999) Factors influencing elevation of intracellular Ca^{2+} in the MCF-10A human mammary epithelial cell line by carcinogenic polycyclic aromatic hydrocarbons. *Mol Carcinog* **25:**48–54.
Upham BL, Weis LM and Trosko JE (1998) Modulated gap junctional intercellular communication as a biomarker of PAH epigenetic toxicity: Structure-function relationship. *Environ Health Perspect* **106(Suppl 4):**975–981.
Zable AC, Favero TG and Abramson JJ (1997) Glutathione modulates ryanodine receptor from skeletal muscle sarcoplasmic reticulum. Evidence for redox regulation of the Ca^{2+} release mechanism. *J Biol Chem* **272:**7069–7077.
Zhao M, Lytton J and Burchiel SW (1996) Inhibition of sarco-endoplasmic reticulum calcium ATPases (SERCA) by polycyclic aromatic hydrocarbons: Lack of evidence for direct effects on cloned rat enzymes. *Int J Immunopharmacol* **18:**589–598.

Send reprint requests to: Dr. Isaac N. Pessah, Department of Molecular Biosciences, School of Veterinary Medicine, University of California Davis, Davis, CA 95616. E-mail: inpessah@ucdavis.edu